Separation and Purification Technology 294 (2022) 121143

Contents lists available at ScienceDirect

Separation and Purification Technology

journal homepage: www.elsevier.com/locate/seppur

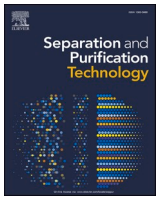

Improving separation efficiency of crystallization by ultrasound-accelerated nucleation: The role of solute diffusion and solvation effect

Menghui Yao [a], Lingyu Wang [a], Shanshan Feng [a], Jiahui Li [a], Chen Fang [a], Suoqing Zhang [a,d], Meitang Jin [b], Li Tong [b], Zhenguo Gao [a], Mingyang Chen [a,b,*], Junbo Gong [a,b,c,*]

[a] State Key Laboratory of Chemical Engineering, School of Chemical Engineering and Technology, Tianjin University, Tianjin 300072, People's Republic of China
[b] Institute of Shaoxing, Tianjin University, Zhejiang, 312300, People's Republic of China
[c] Chemistry and Chemical Engineering Guangdong Laboratory, Shantou 515031, People's Republic of China
[d] North China Pharmaceutical Group Co., Ltd., Shijiazhuang 050000, People's Republic of China

ARTICLE INFO

Keywords:
Ultrasound
Process intensification
Crystallization efficiency
Nucleation kinetics
Computational chemistry

ABSTRACT

The nucleation rate significantly affects the separation and purification efficiency of crystallization. The proper choice of solvent combined with the intensification of ultrasound can further accelerate the nucleation. However, the difference in the ability of ultrasound to promote nucleation in different solvents needs to be considered. Here, the comparative study of crystal nucleation in various solvent environments under ultrasonic and non-ultrasonic conditions was explored. The probability distribution method was employed to better describe the randomness of nucleation events. Over 1500 nucleation induction time experiments of 3,5-dimethoxybenzoic acid in three solvents (ethanol, acetonitrile, acetone) were performed. The results showed that the enhancement on nucleation rate by ultrasound in different solvents ranged from 1% to 116%, which had obvious differences in different solvents. It is revealed that the enhancement degree is mainly affected by solute diffusion and solvation effect. On the one hand, mean square displacement (MSD) analysis of solute molecule demonstrates that, the weaker the diffusion ability of solute in a certain solvent, the more significant the enhancement effect of ultrasound on the nucleation in such solvent system. On the other hand, molecular dynamics (MD) simulation, density functional theory (DFT) calculation and spectroscopy method indicate that the solvation effect is the main factor determining the order of nucleation rate in the three solvents. The stronger the solvation of solvent on the solute, the more difficult the nucleation. So that in our system, the introduction of ultrasound enhances nucleation in each solvent but does not change the order of nucleation rate in the three solvents.

1. Introduction

Crystallization, as a green and efficient separation method, is widely used in the separation and purification processes in the fields of resource recovery, preparation of high-purity crystalline materials, biological purification, removal of harmful substances, production of bio-based products, energy conversion, etc. [1–9].

The separation efficiency of crystallization has been extensively concerned. Nucleation is the first step and important part of crystallization, the nucleation rate greatly affects the period of crystallization and thus has a significant impact on the separation efficiency [10,11]. In recent years, ultrasound is applied as a powerful process intensification method in crystallization processes to improve the crystallization efficiency [12–14]. Especially, the introduction of ultrasound can obviously reduce the induction time and the metastable zone width (MSZW), thereby accelerating the nucleation process [15–17]. In addition, it is worth noting that the solvent, as an indispensable component in solution crystallization, plays a crucial role in the nucleation rate [18–21]. Therefore, if a high crystallization efficiency is required, choosing a suitable solvent to achieve fast nucleation and introducing ultrasound to further enhance nucleation are the two most effective ways. Furthermore, for a certain substance, the difference in the promotion effect of ultrasound on nucleation in different solvents also needs to be considered. However, current studies mainly focus on the enhancement of

* Corresponding authors at: State Key Laboratory of Chemical Engineering, School of Chemical Engineering and Technology, Tianjin University, Tianjin 300072, China (Mingyang Chen), State Key Laboratory of Chemical Engineering, School of Chemical Engineering and Technology, Tianjin University, Tianjin 300072, China (Junbo Gong).
E-mail addresses: chenmingyang@tju.edu.cn (M. Chen), junbo_gong@tju.edu.cn (J. Gong).

https://doi.org/10.1016/j.seppur.2022.121143
Received 3 March 2022; Received in revised form 19 April 2022; Accepted 21 April 2022
Available online 25 April 2022

nucleation by ultrasound in single-solvent systems, concentrating on the effects of different operating parameters such as ultrasound power and supersaturation [22,23]. Moreover, there are also some studies have sought to reveal the mechanism of ultrasonic promotion on nucleation [24,25]. Although these studies have contributed to the understanding of the influence conditions and the intrinsic strengthening mechanism of ultrasound-intensified nucleation, they focus on single-solvent systems. To the best of our knowledge, the effect of ultrasound on nucleation in different solvent systems has not been reported and the strengthening behavior of ultrasound in different solvent systems has been rarely compared. Therefore, this work conducts a comparative study on the strengthening effect of ultrasound on the nucleation of a substance in different solvents, aiming to reveal the similarities and differences in the strengthening effect of ultrasound on nucleation in different solvent systems, as well as the key influencing factors of these phenomena. This study can help to understand the universality, differences and limitations of the strengthening effect of ultrasound on nucleation in various solvents. Moreover, it can help to better utilize ultrasound and guide to achieving high separation efficiency of crystallization.

In this work, three solvent systems (ethanol, acetonitrile and acetone) were selected to conduct crystal nucleation experiments under ultrasonic and non-ultrasonic conditions, to study the similarities and differences of ultrasound strengthening on the nucleation process in different solvents. The nucleation kinetics with/without ultrasound was investigated by the method of probability distribution [26]. This method utilizes the stochastic nature of nucleation, which is beneficial to the overall comparative study of the nucleation process under different conditions. The nucleation induction time experiment under each condition was repeated 80 times, which eventually formed over 1500 experiments to obtain the statistical rule of nucleation process. The enhancement of nucleation rate under different solvents and supersaturations by ultrasound was comparatively studied. Furthermore, computational chemistry (molecular dynamics, density functional theory) and spectroscopy methods were used to reveal the factors that influence the enhancement degree of ultrasound on nucleation in different solvents.

The benzoic acid systems are popular substances for nucleation studies. They have the important benzene ring and carboxylic acid functional groups that most organics have, which play a key role in the nucleation process. 3,5-dimethoxybenzoic acid ($C_9H_{10}O_4$, CAS: 1132–21-4, Fig. 1**(a)**) is a common pharmaceutical intermediate, especially for the synthesis of anticancer drugs [27]. It is a simple and essentially inflexible molecule with only one crystal form reported [28], which avoids the complexity of polymorphism and facilitates the analysis of mechanisms in nucleation studies. The crystal structure of 3,5-dimethoxybenzoic acid is stacked based on the carboxyl dimer of 3,5-dimethoxybenzoic acid molecule **(**Fig. 1**(b))**. Two 3,5-dimethoxybenzoic acid molecules compose a dimer by forming hydrogen bonds (yellow region) between carboxyl groups. Dimers are further connected by hydrogen bonds (purple region) to form the crystal structure of 3,5-dimethoxybenzoic acid. Three solvents including ethanol, acetonitrile and acetone were selected. First, these solvents are widely used in industrial production. Second, they have different hydrogen bond donor and acceptor capacities. Ethanol can act as hydrogen bond donor and acceptor, acetonitrile and acetone can only serve as hydrogen bond acceptor. The selection of solvents with different hydrogen bond donor–acceptor capabilities can make the nucleation research in different solvents more extensive and contrastive.

2. Materials and methods

2.1. Materials

3,5-dimethoxybenzoic acid was purchased from Heowns Chemical Technology Co., Ltd. with mass fraction purity no less than 99.0%. All selected solvents (ethanol, acetonitrile and acetone) were obtained from Jiangtian Chemical Technology Co., Ltd. with mass fraction purity higher than 99.5%. All chemicals were used without further purification.

2.2. Ultrasonic processor

The horn diameter of the ultrasonic processor (JY92-IIN, Scientz, China) was 6 mm, and the ultrasonic irradiation frequency was maintained constant at 20 kHz. For all ultrasonic experiments, pulsed ultrasound (2 s ON and 2 s OFF) was employed, and two types of power including 164 W and 491 W were used.

2.3. Induction time measurement

Induction times were measured using the probability distribution method proposed by Jiang [26]. Here, the nucleation induction times of 3,5-dimethoxybenzoic acid in the three solvents (ethanol, acetonitrile and acetone) at different supersaturation were collected with and without ultrasound. For acetonitrile or acetone, three supersaturations including 1.30, 1.35 and 1.40 were selected for the nucleation experiment. But for ethanol, the nucleation induction time was more than 10 h at the supersaturation of 1.30, which would cause the nucleation experiment to be time-consuming and meaningless. Therefore, the supersaturation of 1.30 was replaced with 1.45, and the other two supersaturations (1.35, 1.40) were consistent with acetonitrile and acetone.

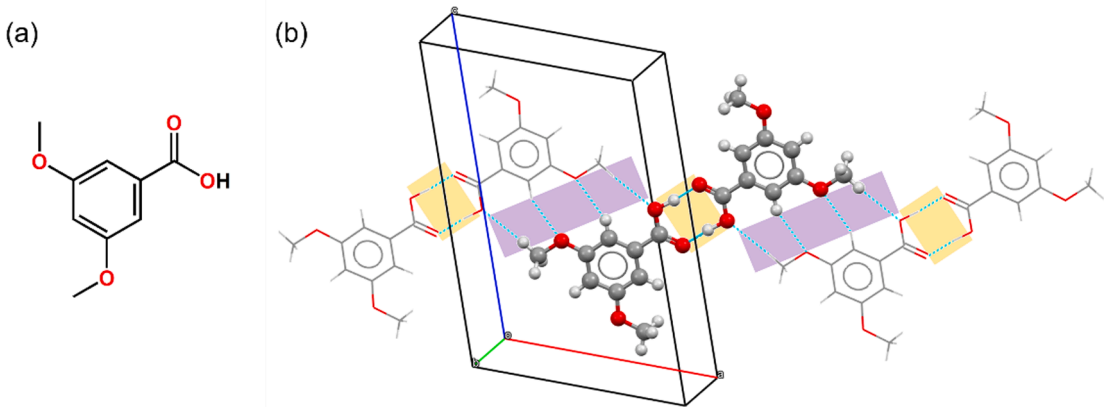

Fig. 1. (a) Molecular structure of 3,5-dimethoxybenzoic acid. (b) Crystal structure of 3,5-dimethoxybenzoic acid based on the carboxyl dimer. White: H atom, grey: C atom, red: O atom. Blue dotted line: hydrogen bond.

2.3.1. With ultrasound

The concentration of the solution was calculated by.

$$S = \frac{x}{x^*} \tag{1}$$

Where S is the supersaturation, x is the actual mole fraction of 3,5-dimethoxybenzoic acid, and x^* is the equilibrium mole fraction at 20 °C, which was reported in our previous work [29] and presented in **Table S2**.

Solutions with different concentrations (corresponding to different supersaturations) were prepared by dissolving appropriate amounts of 3,5-dimethoxybenzoic acid in the respective solvents at 50 °C, which were placed in a 100 ml sealed crystallizer controlled at the constant temperature of 50 °C through a superthermostatic water-circulator bath (CF41, Julabo, Germany). After the solid materials were completely dissolved with agitation provided by a magnetic stirrer (EMS-9A, Ounuo, China), the solution was quickly transferred into five 10 ml glass vials via several preheated syringes equipped with 0.22 μm polytetrafluoroethylene (PTFE) membrane filters. Each vial with a PTFE coated magnetic stirrer bar was dispensed with 4 ml solution and then was sealed with a plastic screw cap. After that, all the vials were stirred in a 50 °C water bath for 1 h.

Next, all vials were quickly transferred from the 50 °C water bath to a 20 °C water bath to start the measurement of induction time. Ultrasound and agitation were applied at the same time which was recorded as the initial time of the induction time measurement. The experimental equipment is shown in Fig. 2. The ultrasound probe was placed at the same distance from each vial in the 20 °C water bath and remained in position throughout the experiment. During the whole experiment, agitation was set at 400 rpm, and the accuracy of temperature was maintained at ± 0.05 °C. The difference between the time when the appearance of crystal and the initial time was recorded as the induction time. After all the vials had nucleated, they were transferred back to the 50 °C water bath to dissolve the crystals into a clear solution. Before the next experiment was performed, all solutions were stirred at 50 °C for 2 h to ensure complete dissolution. Each batch of five vials was subjected to eight temperature cycles (from 50 °C to 20 °C). For each condition, two batches of experiments were carried out to collect 80 sets of induction time data.

Crystals produced under different conditions were immediately separated from the solution by suction filtration. The crystal form was determined by Powder X-ray Diffraction (D/MAX-2500, Rigaku, Japan). In all cases, the solid phase showed consistency with that of raw materials, indicating that there was no polymorphism in all nucleation processes.

2.3.2. Without ultrasound

Compared with the experiment introducing ultrasound, only the agitation was applied when the vials were transferred to the 20 °C water bath, other experimental conditions were the same.

2.4. Nucleation rate calculation

According to the probability distribution method [26], the nucleation probability $P(t)$ at time t in small volumes conforms to the Poisson distribution, which can be expressed as.

$$P(t) = 1 - \exp\left(-JV\left(t - t_g\right)\right) \tag{2}$$

where J is the nucleation rate, V is the volume of solution, t is the induction time measured in the experiment, t_g is the growth time for the formed crystal nucleus to grow to appreciable size, which caused the delay in detection. For a given condition, t_g can be taken as the shortest measured induction time.

The nucleation rate can be obtained by the linear deformation of **Eq. (2)**.

$$-\frac{1}{V}\ln(1 - P(t)) = J\left(t - t_g\right) \tag{3}$$

Plotting $-1/V\ \ln(1-(P(t))$ versus $(t - t_g)$, nucleation rate J can be obtained from the slope of the straight line.

Based on the classical nucleation theory, the nucleation rate is expressed by.

$$J = A\exp\left(\frac{-16\pi\gamma^3 V_s^2}{3k^3T^3}\frac{1}{\ln^2 S}\right) \tag{4}$$

Where A is the pre-exponential factor, γ is the interfacial energy, V_s is the volume of the solute molecule, k is the Boltzmann constant, T is the nucleation temperature and S is the supersaturation. The logarithmic change of **Eq. (4)** can get the following **Eq. (5)**.

$$\ln J = \ln A - \frac{16\pi\gamma^3 V_s^2}{3k^3T^3}\frac{1}{\ln^2 S} \tag{5}$$

Plotting $\ln J$ versus $1/\ln^2 S$, the pre-exponential factor A and interfacial energy γ can be derived from the intercept and slope of the straight line, respectively.

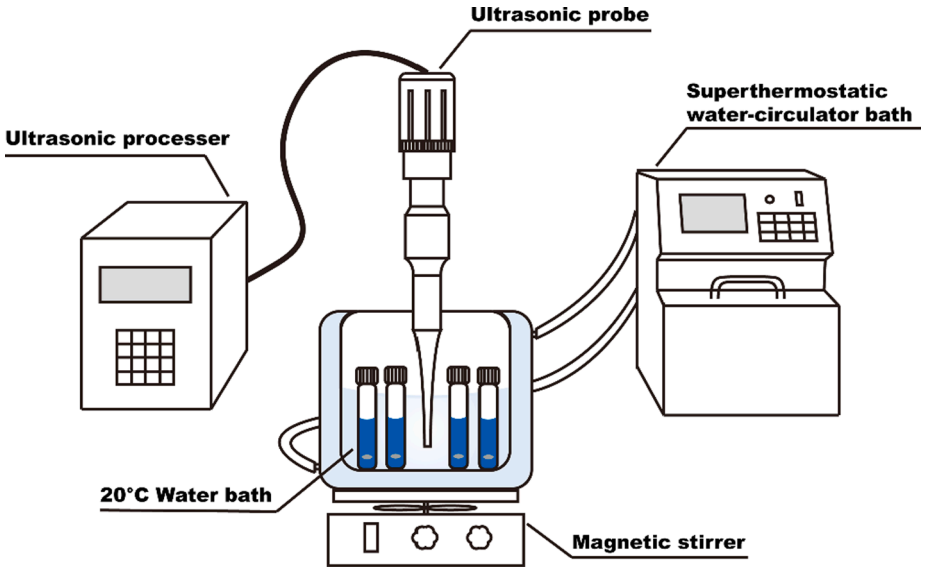

Fig. 2. Experimental equipment for induction time measurement under ultrasound.

2.5. Computational chemistry

2.5.1. Molecular dynamics (MD) simulation

MD simulation was performed using the Forcite module of Materials Studio 8.0 software. The COMPASS force field [30] with the force field assigned charges was used for all the calculations. The detailed procedures to verify the validity of the force field are given in the supporting information. The electrostatic and van der Waals interactions were calculated using Ewald and atom-based summation methods, respectively.

Solvent-solute interaction calculation. For each solute–solvent simulation system, an amorphous cell containing one 3,5-dimethoxybenzoic acid molecule and 500 solvent molecules was constructed. The system was first energy minimized to remove any overlapping of molecules during structure construction, followed by equilibration for a period of 500 ps in the NPT ensemble (constant number of particles, pressure, and temperature). Afterward, another 500 ps in the NPT ensemble was performed for data production and analysis. The Nose thermostat and Berendsen barostat were used to maintain 298 K and 1 atm.

Then the solvent–solute interaction enthalpy can be calculated by:

$$\Delta H_{interaction} = E_{total} - E_{solvent} - E_{solute} \tag{6}$$

Where E_{total} is the total energy of the MD-equilibrated cell with solute and solvent molecules, $E_{solvent}$ is the energy of the MD-equilibrated cell with only solvent molecules after removing the solute molecule, E_{solute} is the energy of the removed solute molecule in its non-relaxed geometry.

Mean square displacement (MSD) analysis. Different from the amorphous cell mentioned above, the number of solute molecules and solvent molecules in each cell here is determined according to the actual solubility ratio of 3, 5-dimethoxybenzoic acid in different solvents. Each solute–solvent system simulation was also carried out with initial energy minimization, followed by 500 ps in the NPT ensemble to allow equilibration and finally a production run of another 500 ps. MSD analysis is based on the first 250 ps of production run in the simulation process.

The diffusion coefficient (D) can be evaluated from the limiting slope of the mean square displacement (MSD) as a function of time [31]:

$$\mathrm{MSD} = \left\langle |r(t) - r(0)|^2 \right\rangle \tag{7}$$

$$D_\alpha = \frac{1}{6N_\alpha} \lim_{t\to\infty} \frac{d}{dt} \sum_{i=1}^{N_\alpha} \left\langle [\boldsymbol{r}_i(t) - \boldsymbol{r}_i(0)]^2 \right\rangle \tag{8}$$

Where N_α is the number of diffusive atoms in the system, $\boldsymbol{r}_i$ denotes the position vector of atom α.

2.5.2. Density functional theory (DFT) calculation

DFT calculation was applied to investigate binding energy in 1:1 solvent–solute dimer by using Gaussian 09 package. The energy was probed at carboxyl site of 3,5-dimethoxybenzoic acid molecule. The initial structure of the 1:1 solute–solvent dimer was extracted from the results of molecular dynamics simulations. The equilibrium geometry of the 1:1 solute–solvent dimer was calculated with a B3LYP-D3 Grimme's functional [32] and Gaussian-type 6-31G (d, p) basis set [33].

The binding energy in a dimer was calculated as follows:

$$\Delta E_{bind} = E_{A-B} - E_A - E_B \tag{9}$$

Where $E_{A\text{-}B}$ is the energy of the dimer A-B, E_A and E_B are the energies of isolated monomers A and B in fully relaxed gas phase geometries. The binding energy was calculated at B3LYP-D3/def2-TZVP level.

2.6. Spectroscopy method

IR spectroscopy of solid and solution were both detected by ATR-FTIR (Alpha, Bruker, Germany), with the wavenumber ranging from 4000 to 400 cm^{-1} and the resolution of 4 cm^{-1}. The concentrations of ethanol solution and acetonitrile solution were 28.39 g/kg and 10.42 g/kg, respectively. Acetone solution was not measured due to the frequency of carbonyl stretching of acetone molecule overlaps with that of 3,5-dimethoxybenzoic acid molecule. All the spectral data were collected at ambient temperature. The solvent spectrum was subtracted from the solution spectrum.

3. Results

3.1. Nucleation in three solvents without ultrasound

The induction time distributions (without ultrasound) of 3,5-dimethoxybenzoic acid in ethanol, acetonitrile and acetone at different supersaturations (S) are displayed in Fig. 3. The nucleation probability $P(t)$ approaches 1 more rapidly, indicating the faster corresponding nucleation rate. Apparently, the nucleation rates in three solvents all improve with increasing supersaturation.

According to **Eq. (3)**, the nucleation rate J can be obtained from the slope of the fitting line by plotting $-1/V \ln(1-(P(t))$ versus $(t - t_g)$, as illustrated in **Fig S1**. The derived nucleation rates in three solvents at different supersaturations are summarized in Table 1. First, the nucleation rate J increases with increasing supersaturation in all solvents. Take ethanol as an example, when the supersaturation increases from 1.35 to 1.40, the nucleation rate improves from 80.45 $m^{-3}s^{-1}$ to 149.75 $m^{-3}s^{-1}$, with an increase of 86%; when the supersaturation increases from 1.40 to 1.45, the nucleation rate improves from 149.75 $m^{-3}s^{-1}$ to 211.58 $m^{-3}s^{-1}$, with an increase of 41%. Secondly, at the same supersaturation, acetone has the fastest nucleation rate, followed by acetonitrile, and ethanol has the slowest one. In other words, under the same nucleation driving force, nucleation becomes more difficult in the order: acetone < acetonitrile < ethanol.

3.2. Nucleation in three solvents with ultrasound

The induction time distributions (with ultrasound) of 3,5-dimethoxybenzoic acid in three solvents at different supersaturations are shown in Fig. 4. With the assistance of ultrasonic irradiation, the induction time distribution in all solvents becomes narrower with increasing supersaturation, indicating that the nucleation rate increases.

The fitting lines of $-1/V \ln(1-(P(t))$ versus $(t - t_g)$ are displayed in **Fig S2.** Among the fittings of nucleation rates (**Figs S1 and S2**), there are some slight deviations. The errors mainly come from several aspects. Firstly, the inherent stochasticity of nucleation can cause errors in the measurement of nucleation rate. This error is unavoidable, but decreases with a more extensive data set of induction times. Secondly, the slightly fluctuating experimental conditions including temperature fluctuations and solvent volatilization, can also lead to measurement error. Moreover, there is an observation error in the appearance of crystals [34]. All nucleation rates with ultrasound are derived from the slope of the straight line and listed in Table 2. Firstly, in the presence of ultrasound, the nucleation rate in all solvents increases with the increase of supersaturation. Take ethanol for example, with the increase of supersaturation from 1.35 to 1.40, the nucleation rate increases by 30%; with the increase of supersaturation from 1.40 to 1.45, the nucleation rate increases by 24%. Secondly, at the same supersaturation, the order of nucleation rate is acetone > acetonitrile > ethanol. Namely, under the same nucleation driving force, the difficulty of nucleation under ultrasonic condition gradually increases in the order: acetone < acetonitrile < ethanol.

3.3. Comparison of nucleation with and without ultrasound

In order to compare the similarities and differences of nucleation under ultrasonic and non-ultrasonic conditions in different solvents, the nucleation rates with and without ultrasound in three solvents (Tables 1 and 2) are plotted in Fig. 5, and the ratios of the nucleation rate with

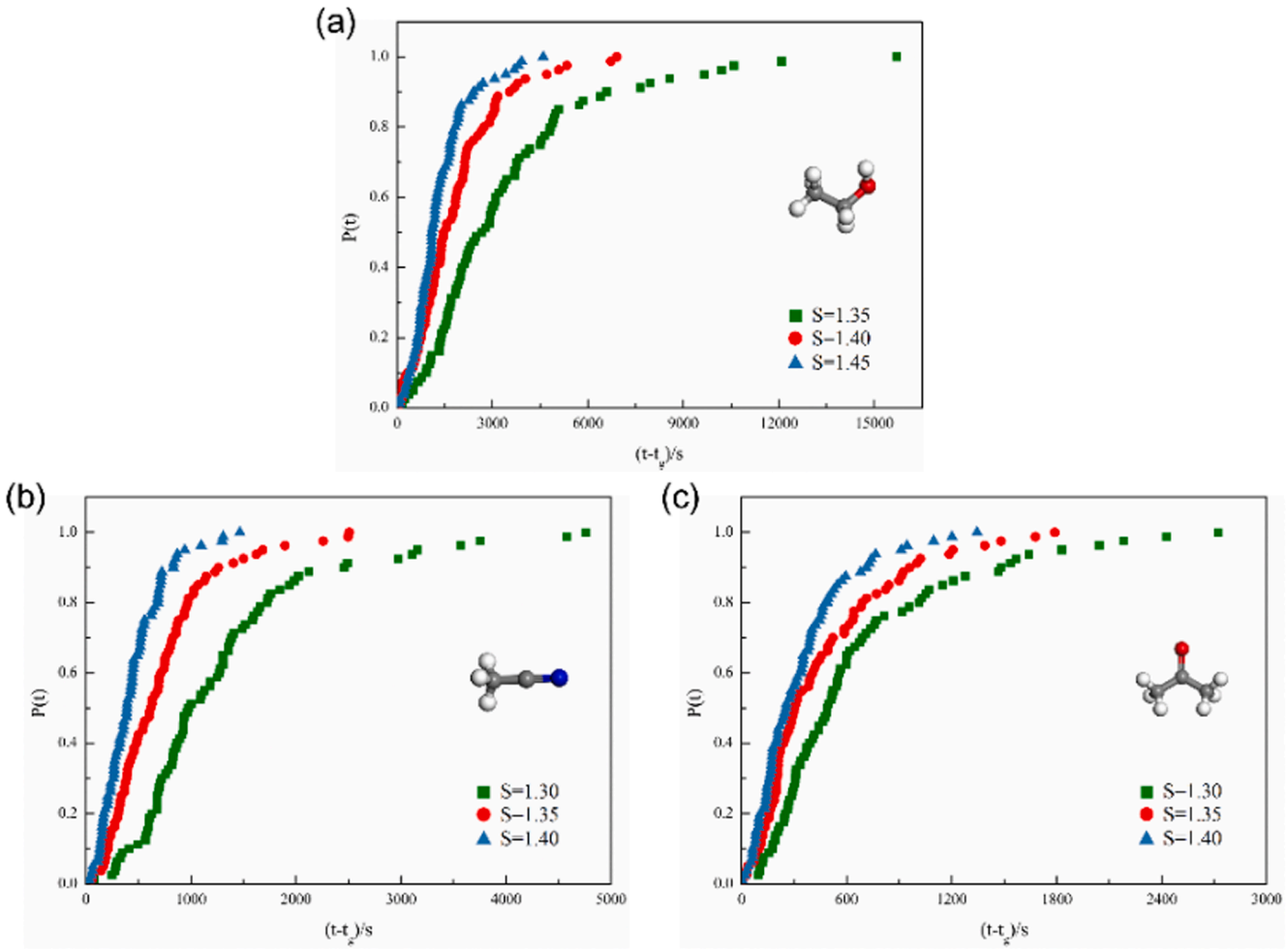

Fig. 3. Induction time distributions (without ultrasound) of 3,5-dimethoxybenzoic acid in (a) ethanol, (b) acetonitrile, (c) acetone.

Table 1
Nucleation rates (without ultrasound) of 3,5-dimethoxybenzoic acid in three solvents at different supersaturations.

supersaturation	nucleation rate J ($m^{-3}s^{-1}$)		
	ethanol	acetonitrile	acetone
1.30	—	218.11	406.71
1.35	80.45	392.46	587.80
1.40	149.75	640.08	816.21
1.45	211.58	—	—

ultrasound to without ultrasound are summarized in **Table S3**. On the whole, ultrasound can accelerate nucleation, especially in ethanol and acetone, but the improvement in acetonitrile is not obvious. It will be discussed in detail in the following section. In addition, ultrasound promotes nucleation more significantly at low supersaturation in all solvents. This was also reported in other studies [17,35].

Besides, according to the **Eq. (5)** derived from classical nucleation theory (CNT), the lines about $\ln J$ versus $1/\ln^2 S$ under ultrasonic and non-ultrasonic conditions are fitted (Fig. 6). On the one hand, the important nucleation parameters including pre-exponential factor A and interfacial energy γ can be obtained from the intercept and slope of the straight line, respectively. The relevant results are listed in **Table S4**. On the other hand, the order of nucleation difficulty in the three solvents can be reflected in Fig. 6. Clearly, whether with or without ultrasound, the required driving force to reach the same nucleation rate increases in the same order: acetone < acetonitrile < ethanol. That is, nucleation in acetone is the easiest, and in ethanol is the most difficult.

4. Discussion

4.1. The role of solute diffusion

According to Section 3.3, the nucleation rates in three solvents increased under the ultrasonic enhancement, indicating that ultrasound can promote the nucleation of 3,5-dimethoxybenzoic acid in all three solvents. Currently, it is generally believed that the effect of ultrasound on nucleation is attributed to the enhancement of molecular diffusion caused by the cavitation phenomena. These phenomena refer to the formation, growth and collapse of bubbles due to the pressure changes in the solution caused by ultrasound [25,35]. The collapse of bubbles causes the generation of shockwaves and acoustic streaming, so that turbulences are created [13,36]. The turbulence enhances the diffusion of solute molecules in the solvent, and then promotes the collision between solute molecules, which is more conducive to forming pre-nucleation molecular clusters [13,37–40]. In this way, ultrasound can accelerate the nucleation of 3,5-dimethoxybenzoic acid in these solvents. Moreover, as mentioned in Section 3.3, ultrasound promotes nucleation more significantly at low supersaturation. At low supersaturation, the relatively low concentration of solute makes the collision of solute molecules relatively difficult, so ultrasound can significantly accelerate the diffusion of solutes molecules to enhance the collision between solute molecules, and then has an obvious promotion on nucleation. Comparatively, at high supersaturation, the concentration of solute is relatively high, and the collision of solute molecules is

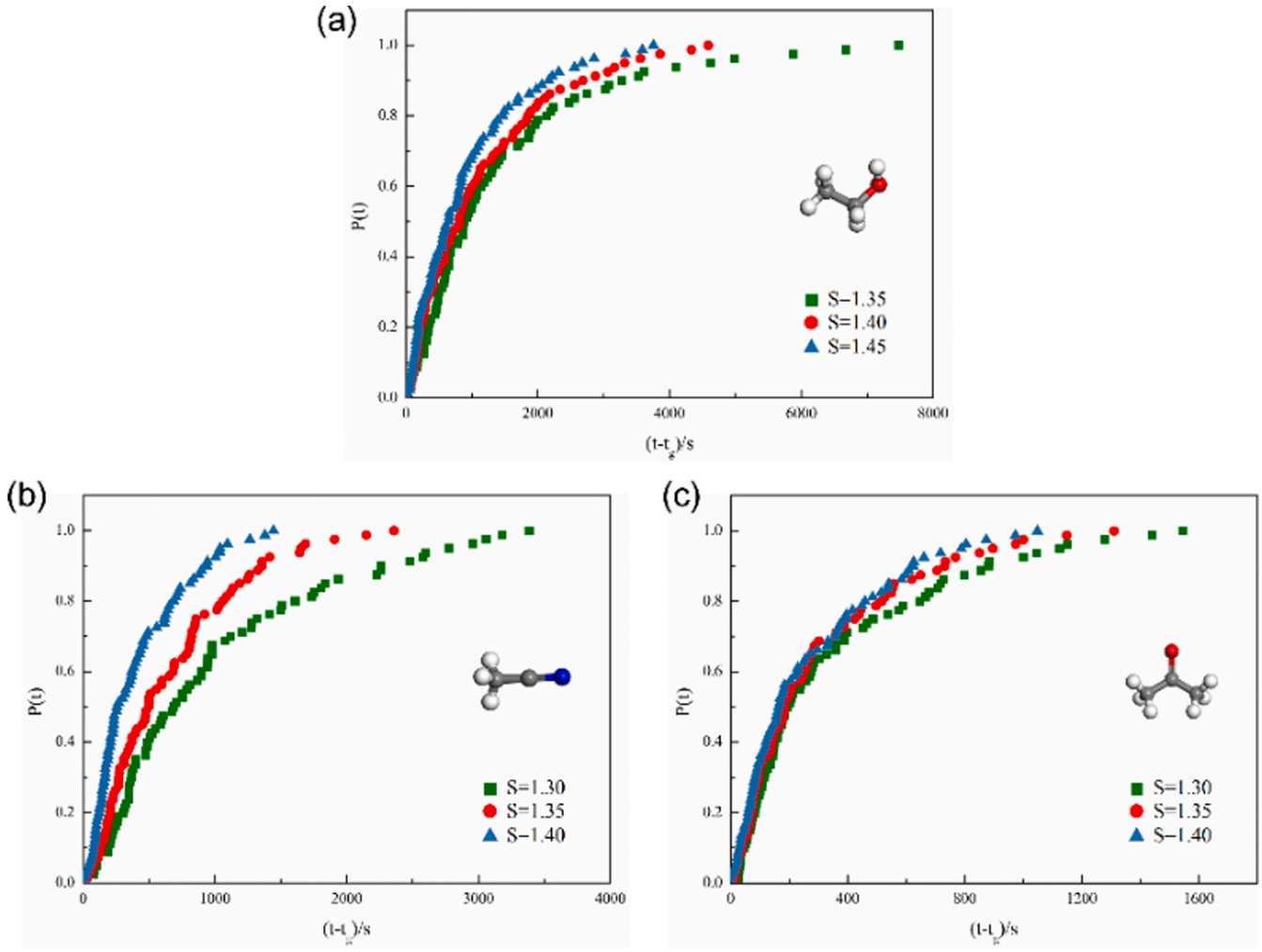

Fig. 4. Induction time distributions (with ultrasound) of 3,5-dimethoxybenzoic acid in (a) ethanol, (b) acetonitrile, (c) acetone. Ultrasonic power is 164 W.

Table 2
Nucleation rates (with ultrasound [a]) of 3,5-dimethoxybenzoic acid in three solvents at different supersaturations.

supersaturation	nucleation rate J ($m^{-3}s^{-1}$)		
	ethanol	acetonitrile	acetone
1.30	—	266.79	697.78
1.35	173.58	415.70	854.12
1.40	225.35	649.25	956.52
1.45	279.21	—	—

[a] Ultrasonic power is 164 W.

relatively easy. Therefore, compared with high supersaturation, the promotion of ultrasound on nucleation is more significant at low supersaturation [17].

It is noteworthy that acetonitrile is different from the other two solvents under the ultrasonic enhancement. As shown in Fig. 5 and **Table S3**, when the supersaturations are 1.35 and 1.40, the nucleation rate in ethanol and acetone is significantly increased by ultrasound, while the rate in acetonitrile is hardly improved. Only when the supersaturation is 1.30, there is a slight increase in nucleation rate in acetonitrile. The reason for the insignificant effect of ultrasound on nucleation in acetonitrile at these supersaturations are discussed. Two possible explanations for this phenomenon are considered. Firstly, the possibility that ultrasonic power is not large enough to be effective is examined. Secondly, the nucleation driving force (supersaturation) may be already so great that it is difficult for the ultrasound to increase the nucleation rate. The second conjecture is based on two phenomena. On the one hand, it is observed that when the supersaturation decreases from 1.40 to 1.30, the nucleation rate in acetonitrile is slightly increased (**Table S3**). On the other hand, as mentioned in Section 3.3, the ultrasound has a stronger promotion on nucleation at low supersaturation, while this effect at high supersaturation is weakened.

According to the above two conjectures, a series of nucleation experiments in acetonitrile with different ultrasonic powers and supersaturations were conducted. Fig. 7 presents the nucleation induction time distributions in acetonitrile under different conditions, and the derived nucleation rates are summarized in Table 3. Comparing Fig. 7**(a)** and Fig. 7**(b)**, even if the ultrasonic power is increased from 164 W to 491 W at high supersaturation (S = 1.35), the induction time distribution does not change obviously and the calculated nucleation rate is not significantly improved as well (Table 3). Comparing Fig. 7**(b)** and Fig. 7**(c)**, when the ultrasonic power is fixed at 164 W but the supersaturation is reduced to 1.25, the induction time distribution is markedly narrowed and the nucleation rate is increased significantly (Table 3). Hence, at the high supersaturation (S = 1.35), even if a strong ultrasonic power (461 W) is used, the nucleation rate is still not obviously changed. In contrast, at the low supersaturation (S = 1.25), only applying a gentle ultrasound (164 W) can achieve a manifest increase in the nucleation rate. It can be concluded that the supersaturation of 1.35 and 1.40 (corresponding nucleation driving force) is already large enough for the acetonitrile system, so that the introduction of ultrasound can hardly increase its nucleation rate. In addition, it also demonstrates that ultrasound can

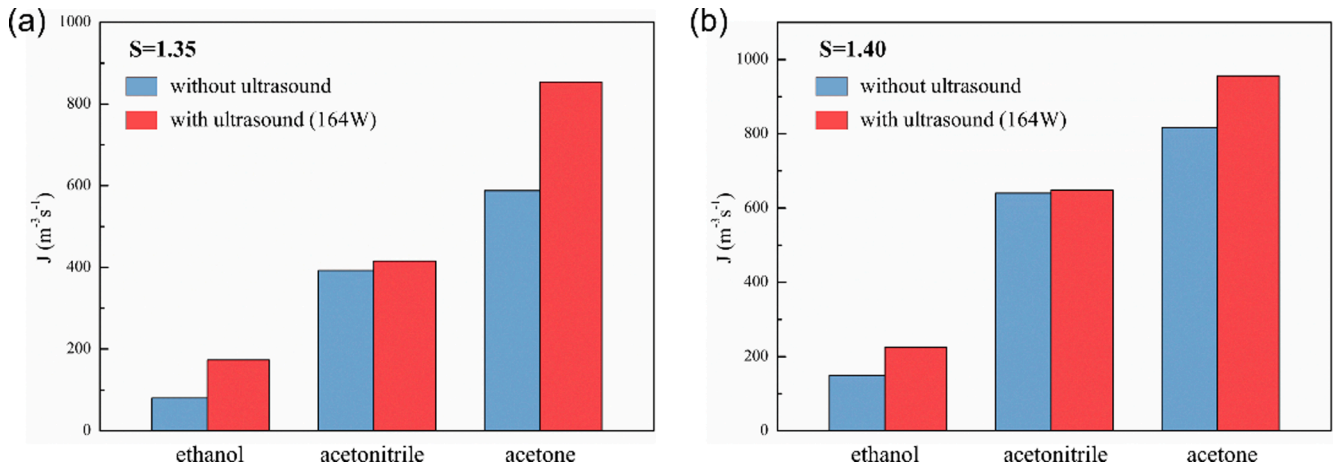

Fig. 5. Nucleation rates with and without ultrasound in three solvents at the supersaturations of (a) 1.35 and (b) 1.40. These two supersaturations are selected for analysis because they are shared by three solvents.

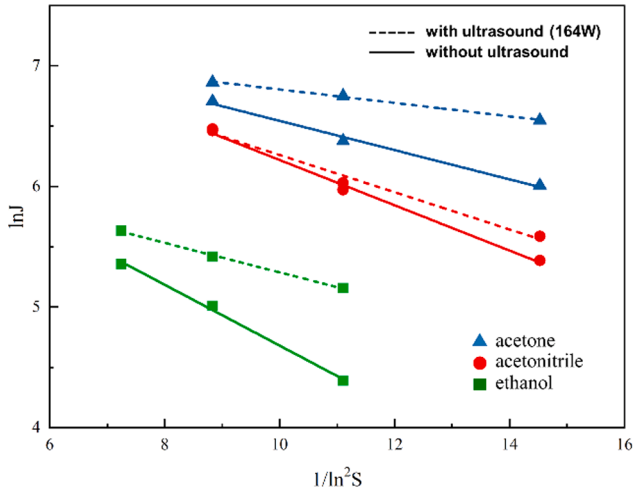

Fig. 6. Relationship between ln$J$ and $1/\ln^2 S$ in three solvents. Dotted line-with ultrasound (164 W), solid line-without ultrasound.

promote nucleation, especially at low supersaturation.

Notably, the supersaturations of 1.35 and 1.40 are large enough for the nucleation in acetonitrile that ultrasound does not significantly promote nucleation, while the nucleation rates in ethanol and acetone can still be obviously improved at these two supersaturations. It is reasonable to speculate that such phenomenon may be related to the difference of diffusion ability of solute molecules in different solvent environments. Because ultrasound accelerates nucleation by enhancing molecular diffusion based on the cavitation phenomena, if the diffusion ability of solute molecules in different solvents is discrepant (at the same supersaturation under non-ultrasonic condition), the enhancement effect of ultrasound may also vary with the solvent species. In this regard, mean square displacement (MSD) analysis based on molecular dynamics (MD) was performed to investigate the diffusion ability of 3,5-dimethoxybenzoic acid molecules in the three solvents. According to **Eqs. (7) and (8)**, the slope of the MSD curve is positively related to the diffusion coefficient. Fig. 8 displays the MSD curve of 3,5-dimethoxybenzoic acid molecules in different solvent systems. Clearly, the diffusion coefficient of 3,5-dimethoxybenzoic acid in acetonitrile is much larger than that in ethanol and acetone. Correspondingly, as shown in Fig. 5, the enhancement of ultrasound on the nucleation in acetonitrile is not manifest compared with the other two solvents. Besides, Fig. 8 demonstrates that the diffusion of solute in acetone is faster than that in ethanol. It can also be found in nucleation experiments that the enhancement effect of ultrasound in ethanol is stronger than that in acetone (Fig. 5 and **Table S3**). In conclusion, if the diffusion ability of solute in a certain solvent is weaker, the enhancement effect of ultrasound on the nucleation in such solvent system will be more significant.

4.2. *The role of solvation effect*

As discussed in Section 4.1, the promotion of ultrasound on nucleation varies with the diffusion ability of solute molecules in different solvents. In this way, ultrasound achieves different degrees of enhancement on nucleation in different solvents. Subsequently, whether ultrasound can change the order of the nucleation difficulty in different solvents is investigated. According to Section 3.3, with or without ultrasound, the nucleation of 3,5-dimethoxybenzoic acid in different solvents becomes increasingly difficult in the same order: acetone < acetonitrile < ethanol (Fig. 6). It means that, in the present case, the application of ultrasound does not change the relative difficulty of nucleation in the three solvents.

For the nucleation process in solution, solute molecules need to overcome the action of solvent molecules (solvation) to form molecular clusters, thereby further forming crystal nuclei. Some recent studies indicated that this solvation may be the key factor affecting the difficulty of nucleation in the solvent [41–43]. In this work, the computational chemistry method and spectroscopy method were utilized to quantify the solvation, to explore the role of solvation in the inability of ultrasound to change the relative difficulty of nucleation in the three solvents.

Molecular dynamics (MD)-calculated interaction enthalpy $\Delta H_{\text{interaction}}$ can generally reflect the strength of solvation [42]. Representative snapshots of three solute–solvent equilibrium systems are shown in Fig. 9. The interaction enthalpies for one 3,5-dimethoxybenzoic acid molecule in equilibrium with three different bulk solvents are given in Table 4. A greater absolute value of enthalpy represents a more significant solvation effect. Among the three solvents, ethanol (-159.36 kJ/mol) has the largest $\Delta H_{\text{interaction}}$ with 3,5-dimethoxybenzoic acid molecule, followed by acetone (−144.09 kJ/mol), and acetonitrile (-121.98 kJ/mol) has the smallest.

Fig. 9 demonstrates all three solvent molecules form hydrogen bonds with the carboxyl group of 3,5-dimethoxybenzoic acid. In fact, carboxyl group is the strongest intermolecular interaction site for 3,5-dimethoxybenzoic acid molecules to assemble into crystals (Fig. 1**(b)**). Therefore, investigating the binding energy between solvent molecule and carboxyl group of 3,5-dimethoxybenzoic acid is crucial for studying the influence of solvents on the nucleation. In this regard, density functional theory (DFT) with higher accuracy was used to calculate the 1:1 solute–solvent

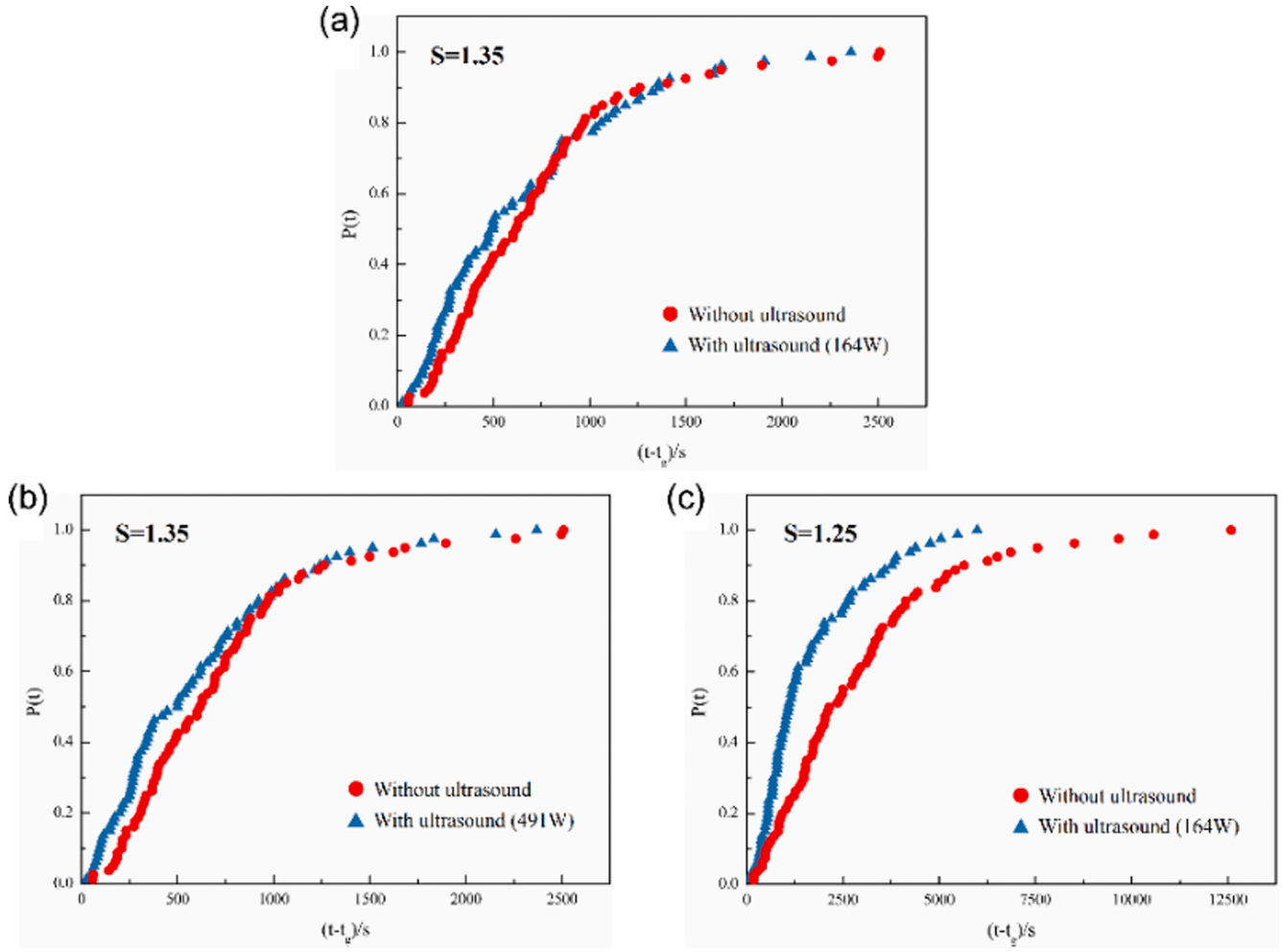

Fig. 7. Induction time distributions in acetonitrile under different conditions. (a) S = 1.35, 164 W power, (b) S = 1.35, 491 W power, and (c) S = 1.25, 164 W power.

Table 3
Comparison of the nucleation rates under different conditions in acetonitrile.

S = 1.35		S = 1.35		S = 1.25	
without ultrasound [a]	392.46	without ultrasound [a]	392.46	without ultrasound [a]	93.38
ultrasound (164 W) [a]	415.70	ultrasound (491 W) [a]	447.60	ultrasound (164 W) [a]	163.83
ratio [b]	1.06	ratio [b]	1.14	ratio [b]	1.75

[a] The unit of nucleation rate is $m^{-3}s^{-1}$.
[b] The ratio of the nucleation rate with ultrasound to without ultrasound.

binding energy ΔE_{bind} at the carboxyl site of 3,5-dimethoxybenzoic acid molecule. The ΔE_{bind} decreases in the order: ethanol (-52.46 kJ/mol) > acetone (-44.96 kJ/mol) > acetonitrile (-36.82 kJ/mol) (Fig. 10).

Infrared spectroscopy (IR) is often selected to study the strength of solvent–solute interaction [41]. Here the shift of the stretching vibration band of carbonyl was utilized to characterize the interaction of solvents with 3,5-dimethoxybenzoic acid. The solid IR spectrum of 3,5-dimethoxybenzoic acid shows strong band for the carbonyl stretching at 1682 cm^{-1} (Fig. 11), which corresponds to the hydrogen-bonded carbonyl group of carboxyl dimer (Fig. 1**(b)**). Compared with solid, the IR spectra of ethanol solution and acetonitrile solution both have an obvious shift of carbonyl frequency. In general, the stronger the solvent interacts, the lower the frequency at which it absorbs [44]. In acetonitrile, the carbonyl peak shifts from 1682 cm^{-1} to 1725 cm^{-1}. In ethanol, two peaks are observed at 1694 cm^{-1} and 1721 cm^{-1}, respectively. This

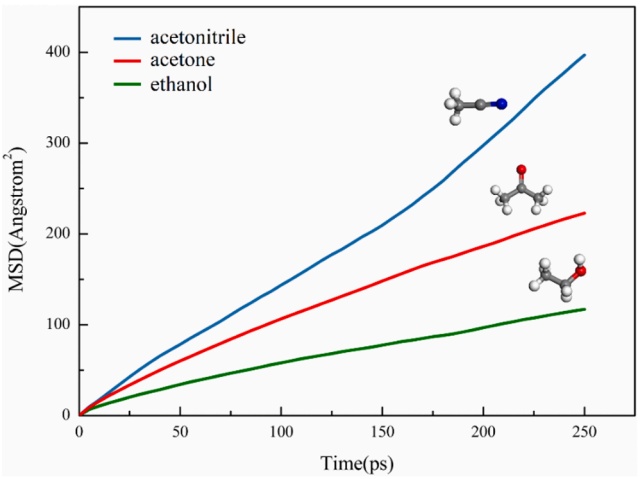

Fig. 8. MSD curve of 3,5-dimethoxybenzoic acid molecule in different solvent systems under non-ultrasonic condition.

difference can be attributed to a solute–solvent hydrogen-bond equilibrium. The low frequency corresponds to the hydrogen-bonded carbonyl group, and the high one corresponds to the non-hydrogen-bonded carbonyl group [45,46]. It can be concluded that 3,5-dimethoxybenzoic acid molecule is more strongly solvated by ethanol, which has a lower frequency of carbonyl stretching.

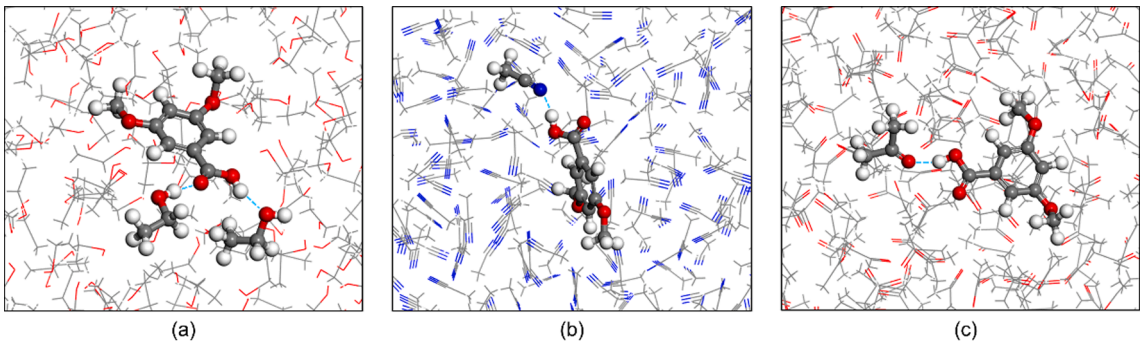

Fig. 9. Representative snapshots of solute–solvent equilibrium systems (a) ethanol, (b) acetonitrile, (c) acetone. Hydrogen bonds are shown as the blue dotted line. White-H atom, grey-C atom, red-O atom, blue-N atom.

Table 4
Solvent-solute interaction enthalpies calculated from MD simulation at 298.15 K.

solvent	ethanol	acetonitrile	acetone
$\Delta H_{interaction}$ (kJ/mol)	−159.36	−121.98	−144.09

Collectively, MD simulation, DFT calculation, and IR spectra all reveal that the solvation of 3,5-dimethoxybenzoic acid molecule in the three solvents is gradually enhanced in the order: acetonitrile < acetone < ethanol. According to the currently accepted view that the strength of solvation dominates the order of nucleation difficulty in different solvents, the nucleation rate (under the same supersaturation) in the three solvents should increase in the following order: ethanol < acetone < acetonitrile. However, the order of actual nucleation rate obtained from the experiment is ethanol < acetonitrile < acetone. The relationship between the actual nucleation rate and the simulation results is displayed in Fig. S3. In other words, "ethanol vs acetonitrile" and "ethanol vs acetone" conform to the above view of solvation effect, while "acetonitrile vs acetone" does not. In fact, the nucleation process is complex and our current understanding of nucleation is still insufficient. Solvation may only be one of the main factors affecting the nucleation difficulty in different solvents. Notably, it was noticed that the solubility of 3,5-dimethoxybenzoic acid in acetonitrile is the smallest, compared with that in ethanol and acetone (**Table S2**). That is to say, even at the same supersaturation (the same nucleation driving force), the solute concentration in acetonitrile solution is the most dilute. It may fundamentally reduce the probability of solute molecules colliding together, which is unfavourable for the formation of pre-nucleation molecular clusters. Therefore, although the solvation in acetone is stronger than that in acetonitrile, the nucleation in acetonitrile is slower. A similar finding was also reported in the nucleation of fenoxycarb [47].

5. Conclusion

In this work, the comparative study of the promotion effect of ultrasound on crystal nucleation in various solvent environments were explored. The introduction of ultrasound can improve the nucleation rates of 3,5-dimethoxybenzoic acid in all solvents, which can significantly enhance the separation efficiency. It is attributed to the cavitation phenomena caused by ultrasound. Such phenomena accelerate the

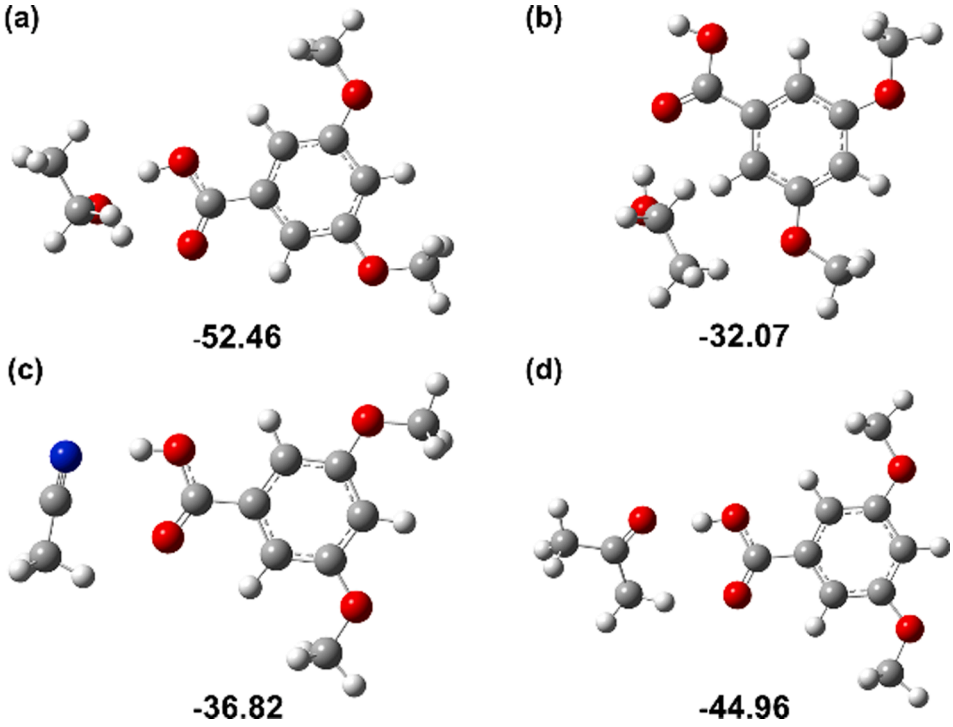

Fig. 10. Optimized geometries and binding energies (in kJ mol^{-1}) of 1:1 solvent–solute dimers (a) ethanol site 1, (b) ethanol site 2, (c) acetonitrile, (d) acetone.

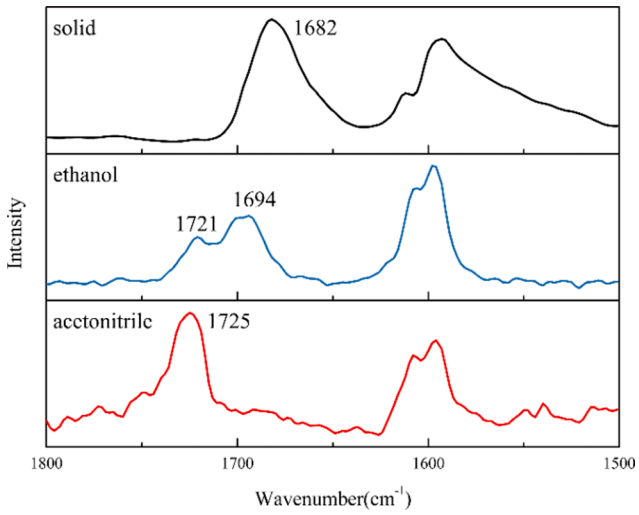

Fig. 11. Solid IR spectrum in comparison with solution spectra of 3,5-dimethoxybenzoic acid.

diffusion and collision of solute molecules. Notably, if the diffusion ability of solute in a certain solvent is weaker, the enhancement effect of ultrasound on the nucleation in such solvent system will be more significant. It was also found that, with or without ultrasound, the nucleation in the three solvents became increasingly difficult in the same order: acetone < acetonitrile < ethanol. MD-calculated solvent–solute interaction enthalpy, DFT 1:1 solvent–solute binding energy and IR spectroscopy indicated that the solvation effect is the main factor that determines the order of nucleation difficulty in different solvents. The stronger the solvation, the more difficult the formation of pre-nucleation molecular clusters, and the slower the nucleation. This study provides guidance for the application of ultrasound in crystallization with different solvent systems to improve the separation efficiency.

CRediT authorship contribution statement

Menghui Yao: Conceptualization, Methodology, Validation, Formal analysis, Investigation, Data curation, Writing – original draft, Writing – review & editing, Visualization. **Lingyu Wang:** Formal analysis, Investigation, Data curation, Validation, Writing – review & editing. **Shanshan Feng:** Investigation, Validation, Data curation. **Jiahui Li:** Investigation, Validation, Data curation. **Chen Fang:** Validation, Writing – review & editing. **Suoqing Zhang:** Investigation, Validation. **Meitang Jin:** Validation. **Li Tong:** Validation. **Zhenguo Gao:** Validation, Writing – review & editing. **Mingyang Chen:** Conceptualization, Resources, Supervision, Project administration, Validation, Writing – original draft, Writing – review & editing. **Junbo Gong:** Funding acquisition, Resources, Supervision, Project administration, Validation, Writing – review & editing.

Declaration of Competing Interest

The authors declare that they have no known competing financial interests or personal relationships that could have appeared to influence the work reported in this paper.

Acknowledgments

The authors are grateful to the financial support of the National Science Foundation of China (Grant No. 22108195), the Key R&D Project of Shandong Province (Grant No. 2020CXGC010506) and the Chemistry and Chemical Engineering Guangdong Laboratory (Grant No. 1912014).

Appendix A. Supplementary material

Supplementary data to this article can be found online at https://doi.org/10.1016/j.seppur.2022.121143.

References

[1] H.S. Demirel, M. Svärd, D. Uysal, Ö.M. Doğan, B.Z. Uysal, K. Forsberg, Antisolvent crystallization of battery grade nickel sulphate hydrate in the processing of lateritic ores, Sep. Purif. Technol. 286 (2022), 120473.
[2] Y. Zhu, L. Ge, L. Chen, C. Chen, Y. Wang, K. Yang, An efficient process for recycle S-valsartan from the racemic coproduct via diastereomeric crystallization by using natural dehydroabietylamine as the enantioselective recognition media, Sep. Purif. Technol. 282 (2022), 120056.
[3] V. Tenberg, M. Sadeghi, A. Seidel-Morgenstern, H. Lorenz, Bypassing thermodynamic limitations in the Crystallization-based separation of solid solutions, Sep. Purif. Technol. 283 (2022), 120169.
[4] P. Das, S. Dutta, K.K. Singh, Insights into membrane crystallization: A sustainable tool for value added product recovery from effluent streams, Sep. Purif. Technol. 257 (2021), 117666.
[5] W. Chen, X. Li, M. Guo, F.J. Link, S.S. Ramli, J. Ouyang, I. Rosbottom, J.Y.Y. Heng, Biopurification of monoclonal antibody (mAb) through crystallisation, Sep. Purif. Technol. 263 (2021), 118358.
[6] A. Kasturi, J. Gabitto, C. Tsouris, R. Custelcean, Carbon dioxide capture with aqueous amino acids: Mechanistic study of amino acid regeneration by guanidine crystallization and process intensification, Sep. Purif. Technol. 271 (2021), 118839.
[7] J.-Y. Lin, N.N.N. Mahasti, Y.-H. Huang, Fluidized-bed crystallization of barium perborate for continuous boron removal from concentrated solution: Supersaturation as a master variable, Sep. Purif. Technol. 278 (2021) 119588.
[8] W. Chen, T.N.H. Cheng, L.F. Khaw, X. Li, H. Yang, J. Ouyang, J.Y.Y. Heng, Protein purification with nanoparticle-enhanced crystallisation, Sep. Purif. Technol. 255 (2021), 117384.
[9] E.D. Gomes, A.E. Rodrigues, Crystallization of vanillin from kraft lignin oxidation, Sep. Purif. Technol. 247 (2020), 116977.
[10] J.V. Parambil, M. Schaepertoens, D.R. Williams, J.Y.Y. Heng, Effects of Oscillatory Flow on the Nucleation and Crystallization of Insulin, Cryst. Growth Des. 11 (10) (2011) 4353–4359.
[11] J. Wang, F. Li, R. Lakerveld, Process intensification for pharmaceutical crystallization, Chem. Eng. Process.: Process Intesif. 127 (2018) 111–126.
[12] J.R.G. Sander, B.W. Zeiger, K.S. Suslick, Sonocrystallization and sonofragmentation, Ultrason. Sonochem. 21 (6) (2014) 1908–1915.
[13] J. Jordens, B. Gielen, C. Xiouras, M.N. Hussain, G.D. Stefanidis, L.C.J. Thomassen, L. Braeken, T., Van Gerven, Sonocrystallisation: Observations, theories and guidelines, Chem. Eng. Process.: Process Intesif. 139 (2019) 130–154.
[14] H.U. Rodríguez Vera, F. Baillon, F. Espitalier, P. Accart, O. Louisnard, Crystallization of α-glycine by anti-solvent assisted by ultrasound, Ultrason. Sonochem. 58 (2019), 104671.
[15] N. Lyczko, F. Espitalier, O. Louisnard, J. Schwartzentruber, Effect of ultrasound on the induction time and the metastable zone widths of potassium sulphate, Chem. Eng. J. 86 (3) (2002) 233–241.
[16] M.N. Hussain, J. Jordens, J.J. John, L. Braeken, T. Van Gerven, Enhancing pharmaceutical crystallization in a flow crystallizer with ultrasound: Anti-solvent crystallization, Ultrason. Sonochem. 59 (2019) 104743.
[17] S.V. Dalvi, M.D. Yadav, Effect of ultrasound and stabilizers on nucleation kinetics of curcumin during liquid antisolvent precipitation, Ultrason. Sonochem. 24 (2015) 114–122.
[18] F.L. Nordström, M. Svärd, Å.C. Rasmuson, Primary nucleation of salicylamide: the influence of process conditions and solvent on the metastable zone width, CrystEngComm. 15 (2013) 7285–7297.
[19] T.D. Turner, D.M.C. Corzo, D. Toroz, A. Curtis, M.M. Dos Santos, R.B. Hammond, X. Lai, K.J. Roberts, The influence of solution environment on the nucleation kinetics and crystallisability of para-aminobenzoic acid, Phys. Chem. Chem. Phys. 18 (39) (2016) 27507–27520.
[20] S. Xu, Y. Bu, S. Jiang, P. Yang, Y. Wang, Insights into the Role of Solvents in Nucleation Kinetics of Glutaric Acid from Metastable Zone Widths, Ind. Eng. Chem. Res. 60 (7) (2021) 3073–3082.
[21] J. Ouyang, X. Xing, J. Chen, L. Zhou, Z. Liu, J.Y.Y. Heng, Effects of solvent, supersaturation ratio and silica template on morphology and polymorph evolution of vanillin during swift cooling crystallization, Particuology 65 (2022) 93–104.
[22] T. Hazi Mastan, M. Lenka, D. Sarkar, Nucleation kinetics from metastable zone widths for sonocrystallization of l-phenylalanine, Ultrason. Sonochem. 36 (2017) 497–506.
[23] X. Zhong, C. Huang, L. Chen, Q. Yang, Y. Huang, Effect of ultrasound on the kinetics of anti-solvent crystallization of sucrose, Ultrason. Sonochem. 82 (2022), 105886.
[24] A.H. Batghare, K. Roy, V.S. Moholkar, Investigations in physical mechanism of ultrasound-assisted antisolvent batch crystallization of lactose monohydrate from aqueous solutions, Ultrason. Sonochem. 67 (2020), 105127.
[25] S. Nalesso, M.J. Bussemaker, R.P. Sear, M. Hodnett, J. Lee, A review on possible mechanisms of sonocrystallisation in solution, Ultrason. Sonochem. 57 (2019) 125–138.
[26] S. Jiang, J.H. ter Horst, Crystal Nucleation Rates from Probability Distributions of Induction Times, Cryst. Growth Des. 11 (1) (2011) 256–261.

[27] C.M. John, S. Arockiasamy, Syringic acid (4-hydroxy-3,5-dimethoxybenzoic acid) inhibits adipogenesis and promotes lipolysis in 3T3-L1 adipocytes, Nat. Prod. Res. 34 (2020) 3432–3436.
[28] D.E. Lynch, G. Smith, K.A. Byriel, C.H.L. Kennard, {3,5-Dimethoxybenzoic acid and the second polymorph of the 2:1 adduct of 3,5-dinitrobenzoic acid with ethylenediamine}, Acta Crystallogr. C 50 (1994) 1259–1262.
[29] S. Feng, M. Yao, S. Guo, Y. Liu, H. Peng, Y. Ma, P. Shi, J. Gong, M. Chen, Understanding the solid-liquid phase equilibrium of 3,5-dimethoxybenzoic acid in thirteen pure solvents by thermodynamic analysis and molecular simulation, J. Mol. Liq. 332 (2021), 115882.
[30] H. Sun, COMPASS: An ab Initio Force-Field Optimized for Condensed-Phase Applications-Overview with Details on Alkane and Benzene Compounds, J. Phys. Chem. B 102 (1998) 7338–7364.
[31] M. Meunier, Diffusion coefficients of small gas molecules in amorphouscis cis-1,4-polybutadiene estimated by molecular dynamics simulations, J. Chem. Phys. 123 (2005), 134906.
[32] A.D. Becke, Density-functional thermochemistry. III. The role of exact exchange, J. Chem. Phys. 98 (7) (1993) 5648–5652.
[33] V.A. Rassolov, M.A. Ratner, J.A. Pople, P.C. Redfern, L.A. Curtiss, 6–31G* basis set for third-row atoms, J. Comput. Chem. 22 (9) (2001) 976–984.
[34] Y. Xiao, S.K. Tang, H. Hao, R.J. Davey, T. Vetter, Quantifying the Inherent Uncertainty Associated with Nucleation Rates Estimated from Induction Time Data Measured in Small Volumes, Cryst. Growth Des. 17 (5) (2017) 2852–2863.
[35] C. Fang, W. Tang, S. Wu, J. Wang, Z. Gao, J. Gong, Ultrasound-assisted intensified crystallization of L-glutamic acid: Crystal nucleation and polymorph transformation, Ultrason. Sonochem. 68 (2020) 105227.
[36] V.S. Nalajala, V.S. Moholkar, Investigations in the physical mechanism of sonocrystallization, Ultrason. Sonochem. 18 (1) (2011) 345–355.
[37] Z. Guo, A.G. Jones, N. Li, The effect of ultrasound on the homogeneous nucleation of BaSO4 during reactive crystallization, Chem. Eng. Sci. 61 (2006) 1617–1626.
[38] Z.i. Zhang, D.-W. Sun, Z. Zhu, L. Cheng, Enhancement of Crystallization Processes by Power Ultrasound: Current State-of-the-Art and Research Advances, Compr. Rev. Food Sci. F. 14 (4) (2015) 303–316.
[39] S.V. Dalvi, R.N. Dave, Analysis of nucleation kinetics of poorly water-soluble drugs in presence of ultrasound and hydroxypropyl methyl cellulose during antisolvent precipitation, Int. J. Pharmaceut. 387 (1-2) (2010) 172–179.
[40] R. Prasad, S.V. Dalvi, Sonocrystallization: Monitoring and controlling crystallization using ultrasound, Chem. Eng. Sci. 226 (2020), 115911.
[41] D. Khamar, J. Zeglinski, D. Mealey, Å.C. Rasmuson, Investigating the Role of Solvent-Solute Interaction in Crystal Nucleation of Salicylic Acid from Organic Solvents, J. Am. Chem. Soc. 136 (33) (2014) 11664–11673.
[42] J. Zeglinski, M. Kuhs, D. Khamar, A.C. Hegarty, R.K. Devi, Å.C. Rasmuson, Crystal Nucleation of Tolbutamide in Solution: Relationship to Solvent, Solute Conformation, and Solution Structure, Chem.-Eur. J. 24 (2018) 4916–4926.
[43] R.A. Sullivan, R.J. Davey, G. Sadiq, G. Dent, K.R. Back, J.H. ter Horst, D. Toroz, R. B. Hammond, Revealing the Roles of Desolvation and Molecular Self-Assembly in Crystal Nucleation from Solution: Benzoic and p-Aminobenzoic Acids, Cryst. Growth Des. 14 (5) (2014) 2689–2696.
[44] D. Mealey, J. Zeglinski, D. Khamar, Å.C. Rasmuson, Influence of solvent on crystal nucleation of risperidone, Faraday Discuss. 179 (2015) 309–328.
[45] P. Shi, S. Xu, Y. Ma, W. Tang, F. Zhang, J. Wang, J. Gong, Probing the structural pathway of conformational polymorph nucleation by comparing a series of α, ω-alkanedicarboxylic acids, IUCrJ 7 (2020) 422–433.
[46] W. Du, A.J. Cruz-Cabeza, S. Woutersen, R.J. Davey, Q. Yin, Can the study of self-assembly in solution lead to a good model for the nucleation pathway? The case of tolfenamic acid, Chem. Sci. 6 (6) (2015) 3515–3524.
[47] J. Zeglinski, M. Kuhs, K.R. Devi, D. Khamar, A.C. Hegarty, D. Thompson, Å. C. Rasmuson, Probing Crystal Nucleation of Fenoxycarb from Solution through the Effect of Solvent, Cryst. Growth Des. 19 (4) (2019) 2037–2049.